Phases of Holographic Nuclear matter , Instanton crystals

>

Nordita October 2022

Matti Jarvinen, V. Kaplunovsky , D. Melnikov

Nuclear matter in Large Nc

- **Holography** obviously associates with **large Nc**.
- Do we expect that the phase of **nuclear matter** in large Nc and finite Nc are the same?
- It is believed the nuclקar matter in nature (Nc=3) is in a liquid phase. Is it the same at large Nc?
- Is the behavior **universal** or model dependent

Nuclear matter in Large Nc

- Let's take an analogy from condensed matter – some atoms that attract at large and intermediate distances but have a hard core-repulsion at short ones.
- The kinetic energy

$$\boxed{K \sim \frac{\pi^2\hbar^2}{2M_{\mathrm{atom}}(\mathrm{well\ diameter})^2}}$$

- The ratio between the kinetic and potential energies at T=0 p=0 is given by the deBour parameter

$$\boxed{\frac{K}{U} \approx 11\Lambda_B^2\,, \qquad \Lambda_B = \frac{\hbar}{r_c\sqrt{2M\epsilon}}}$$

and where

r_c hard core radius ε is the maximal depth of the potential.

Limitations of Large N_c and holography

When Λ_B exceeds 0.2-0.3 the crystal melts.

For example,

- Helium has $\Lambda_B = 0.306$, $K/U \approx 1$ quantum liquid
- Neon has $\Lambda_B = 0.063$, $K/U \approx 0.05$; a crystalline solid
- For large Nc the leading nuclear potential behaves as

$$\begin{aligned} V(\vec{r}, I_1, I_2, J_2, J_2; N_c) \;=\; & N_c \times A_C(r) + N_c \times A_S(r)(\mathbf{I}_1\mathbf{I}_2)(\mathbf{J}_1\mathbf{J}_2) \\ & + N_c \times A_T(r)(\mathbf{I}_1\mathbf{I}_2)\big[3(\mathbf{n}\mathbf{J}_1)(\mathbf{n}\mathbf{J}_2) - (\mathbf{J} \\ & + O(1/N_c). \end{aligned}$$

- Since the well diameter is Nc independent and the mass M scales as~Nc

$$\frac{K}{U} \propto \frac{N_c^{-1}}{N_c^{+1}} = \frac{1}{N_c^2}.$$

Limitations of Large N_c and holography

- The maximal depth of the nuclear potential is ~ 100 Mev so we take it to be $\epsilon \sim N_c \times 30$, the mass scales as

$M_N \sim N_c \times 300 \ \mathrm{MeV}$. $r_c \sim 0.7$

Consequently

$$\boxed{\Lambda_B = \frac{\hbar}{r_c\sqrt{2M\epsilon}} \sim \frac{2}{N_c} \Longrightarrow \frac{K}{U} \sim \frac{45}{N_c^2}}$$

Hence the critical value is $N_c=8$

Liquid nuclear matter Nc<8

Solid Nuclear matter Nc>8

Holographic nuclear matter is a crystal of baryons that are flavor instantons

Baryons as Instantons in the SS model (review)

- In the SS model the **baryon** takes the form of an **instanton** in the 5d $U(N_f)$ gauge theory.

D4 wrapped on S^4 $\simeq$ instanton on D8 $\simeq$ Skyrmion

[Witten, Gross-Ooguri 1998] [Atiyah-Manton 1989] [Skyrme 1961]

Realization of Atiyah-Manton: $U(x^\mu) \equiv P \exp\left\{-\int_{-\infty}^{\infty} dz\, A_z(x^\mu, z)\right\}$

Skyrmion **Instanton**

- The instanton is a **BPST**-like instanton in the (x_i,z) 4d curved space. In the leading order in λ it is exact.

baryon # **Instanton #**

$$N_B = \frac{1}{8\pi^2}\int \mathrm{tr} F \wedge F$$

Baryons in the generalized SSW model

- The probe brane world volume 9d → 5d upon

Integration over the S^4. The **5d DBI+ CS** is
approximated

$$S = S_{\rm YM} + S_{\rm CS} \ ,$$

$$S_{\rm YM} = -\kappa \int d^4x dz \ {\rm tr}\left[\frac{1}{2} h(z)\mathcal{F}_{\mu\nu}^2 + k(z)\mathcal{F}_{\mu}^2\right.$$

$$S_{\rm CS} = \frac{N_c}{\ } \int \omega_5^{U(N_f)}(\mathcal{A}) \ .$$

where $h(z) = (1+z^2)^{-1/3} \ , \quad k(z) = 1+z^2$

Baryons in the Sakai Sugimoto model

- Upon introducing the CS term (next to leading in 1/λ), the instanton is a source of the U(1) gauge field that can be solved exactly.

- Rescaling the coordinates and the gauge fields, one determines the size of the baryon by minimizing its energy

$$
\begin{aligned}
M &= 8\pi^2\kappa + \kappa\lambda^{-1}\int d^3x dz\left[-\frac{z^2}{6}\,\mathrm{tr}(F_{ij})^2 + z^2\,\mathrm{tr}(F_{iz})^2\right] \\
&\quad - \frac{1}{2}\kappa\lambda^{-1}\int d^3x dz\left[(\partial_M \widehat{A}_0)^2 + \frac{1}{32\pi^2 a}\widehat{A}_0\,\epsilon_{MNPQ}\,\mathrm{tr}(F_{MN}F_{PQ})\right] + \mathcal{O}(\lambda^{-1}) \\
&= 8\pi^2\kappa\left[1 + \lambda^{-1}\left(\frac{\rho^2}{6} + \frac{1}{320\pi^4 a^2}\frac{1}{\rho^2} + \frac{Z^2}{3}\right) + \mathcal{O}(\lambda^{-2})\right] \; .
\end{aligned}
$$

Baryon (Instanton) size

- For $N_f = 2$ the **SU(2)** yields a **rising potential**
- The coupling to the **U(1)** via the CS term has a **run away potential .**
- The combined effect

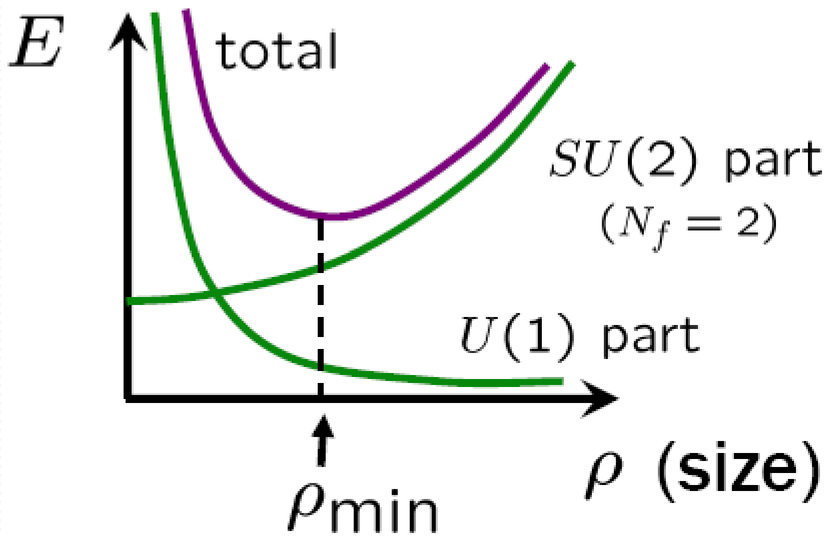

"stable" size but unfortunately on the order of $\lambda^{-1/2}$ so stringy effects cannot be neglected in the large λ limit.

Baryons in the Sakai Sugimoto model

- One decomposes the flavor gauge fields to SU(2) and U(1)
- In a 1/λ expansion the leading term is the YM action
- Ignoring the curvature the solution of the SU(2) gauge field with baryon #= instanton #=1 is the **BPST instanton**

$$\boxed{A_M(x) = -i f(\xi)\, g \partial_M g^{-1} \,,}$$

$$f(\xi) = \frac{\xi^2}{\xi^2 + \rho^2} \,, \quad \xi = \sqrt{(\vec{x} - \vec{X})^2 + (z - Z)^2} \,,$$

$$g(x) = \frac{(z - Z) - i(\vec{x} - \vec{X}) \cdot \vec{\tau}}{\xi} \,,$$

On holographic nuclear interaction

- In real life, the nucleon has a fairly **large radius** ,

$$\boxed{R_{nucleon} \sim 4/M_{\rho meson}.}$$

- But in the holographic nuclear physics with $\lambda \gg 1$,

$$\boxed{R_{baryon} \sim 1/\left(\sqrt{\lambda}\; M\right),}$$

- *Thanks to this hierarchy, the nuclear forces between* two baryons at distance r from each other fall into

3 distinct zones

Zones of the nuclear interaction

- The **3 zones** in the **nucleon-nucleon interaction**

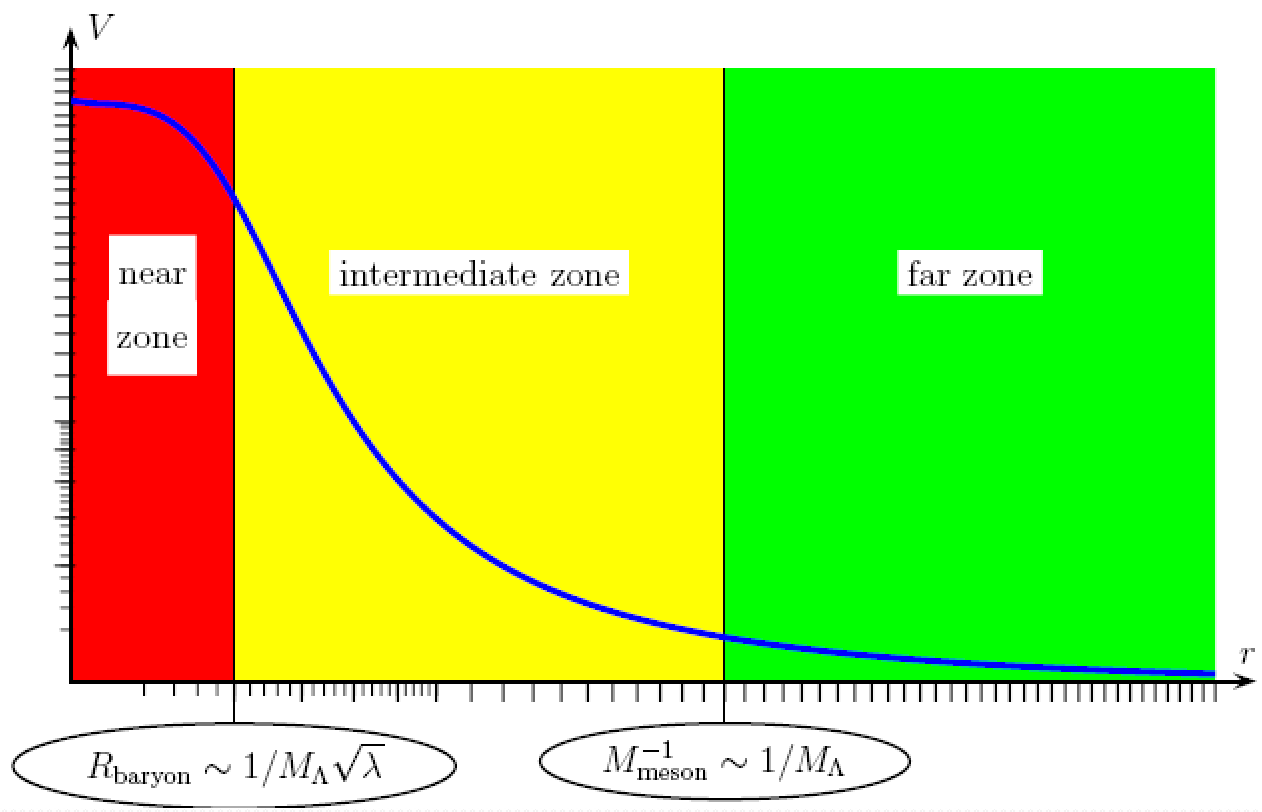

Near Zone of the nuclear interaction

- In the **near zone** **r <Rbaryon ≪ (1/M),** the two baryons overlap and cannot be approximated as two separate instantons ; instead, we need the **ADHM solution of instanton #= 2** in all its complicated glory. We solved it in one dimension.

- On the other hand, *in the near zone, the nuclear force is 5D: the curvature of the fifth* dimension z does not matter at short distances, so we may treat the U(2) gauge fields as living in a flat 5D space-time.

Far Zone of the nuclear interaction

- In the **far zone r > (1/M) ≫ Rbaryon** poses the opposite situation: The curvature of the 5D -> **z–dependence of the gauge coupling** becomes very important at large distances.
- At the same time, the two baryons become **well-separated instantons** which may be treated as **point sources** of the 5D abelian field . In 4D terms, the baryons act as point sources for all the **massive vector mesons** comprising the 5D vector field Aμ(x, z), hence the nuclear force in the far zone is the sum of 4D **Yukawa forces**

$$V(r) = \frac{N_c^2}{4\kappa} \sum_n |\psi_n(z=0)|^2 \times \frac{e^{-m_n r}}{4\pi r}$$

Intermediate Zone of the nuclear interaction

- In the **intermediate zone $R_{baryon} \ll r \ll (1/M)$,** we have the best of both situations:

- The baryons do not overlap much and the fifth dimension is approximately flat.
- At first blush, the nuclear force in this zone is simply the 5D Coulomb force between two point

$$\boxed{V(r) = \frac{N_c^2}{4\kappa} \times \frac{1}{4\pi^2 r^2} = \frac{27\pi N_c}{2\lambda M_\Lambda} \times \frac{1}{r^2}}$$

Attraction versus repulsion

- In the generalized model the story is different.
- Indeed the 5d effective action for A_M and ϕ is

$$S_{5d} = \int d^4x dw \left[N_c \lambda M_\Lambda [\frac{u}{u_0} tr[F_{MN}^2 + \frac{u^9}{u_0^9} \frac{1}{1-\zeta^{-3}} (\partial_M \phi)^2] - N_c [\phi (Tr F_{MN}^2) -$$

- For instantons F=*F so there is a competition between

repulsion — A TrF*F

attraction — ϕTr F^2

- The attraction potential also behaves as

$$V_{scalar} \sim 1/r^2$$

Attraction versus repulsion

- The ratio between the **attraction** and **repulsion** in the intermediate zone is

$$\boxed{C_{a/r} \equiv \frac{-V^{\text{attractive}}}{V^{\text{repulsive}}} = \frac{1}{9} \times \left(1 - \zeta^{-3}\right),}$$

- $\zeta = u_o / u_{KK}$

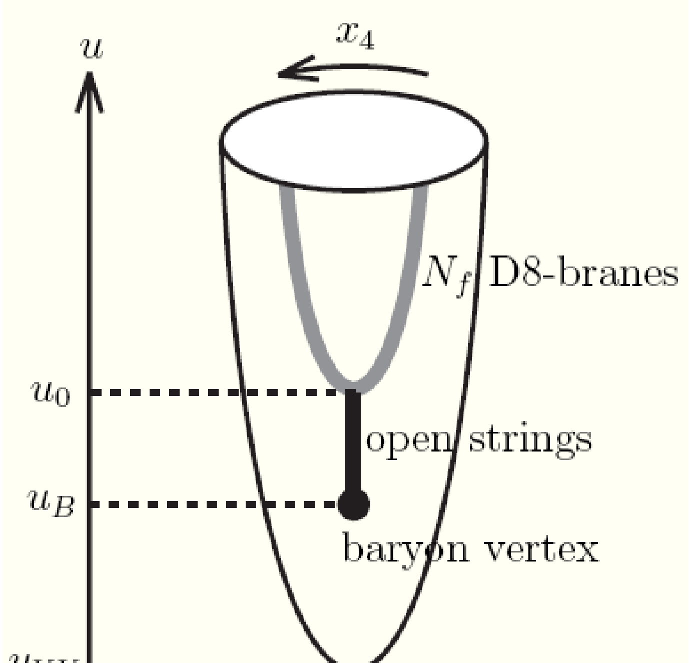

Instanton lattice: basic three dimensional setup

- We consider a 3d system of point-like SU(2) instantons located at the same value of the holographic coordinate.
- Each instanton is characterized by $(\vec{X}_n, y_n)$
- The **position** ~X = (X1;X2;X3)
- The **SU(2) orientation** expressed in terms of the unimodular quaternion (y1; y2; y3; y4)
- The vectors in the quaternion space are denoted by:
- 1 = (1; 0; 0; 0), i = (0; 1; 0; 0), j = (0; 0; 1; 0), and k = (0; 0; 0;
- We also use the representation of the quaternions as a 2x2 matrices,

$$y = y^4 + i\tau^j y^j \qquad \mathrm{tr}(y^\dagger y) = 2$$

The two body forece between instantons

- In holographic nuclear physics, like in real life, besides the two-body nuclear forces due to meson exchanges, there are significant three-body and probably also **higher number-body forces**

$$\hat{H}_{\text{nucleus}} = \sum_{n=1}^{A} \hat{H}^{1\,\text{body}}(n) + \frac{1}{2} \sum_{\substack{\text{different}\\ m,n=1,\dots A}} \hat{H}^{2\,\text{body}}(m,n) + \frac{1}{6} \sum_{\substack{\text{different}\\ \ell,m,n=1,\dots A}} \hat{H}^{3\,\text{body}}(\ell,m,n) + \cdots$$

- In the **low-density regime** of baryons separated by distances much larger then their radii, the **two-body forces dominate the interactions**, while the multi-body forces are smaller by powers of (radius/distance)^2 .

Two body forece between instantons

- We use a **two-body potential** motivated by the Witten-Sakai-Sugimoto model. Assuming that the separation $|X_m - X_n|$ between the instantons n and m satisfies

$$\boxed{\frac{1}{M\sqrt{\lambda}} \ll |X_m - X_n| \ll \frac{1}{M}}$$

coupling constant

Kaluza Klein scale

- The lower limit arises from the instanton size and the upper limit from neglecting curvature corrections in the AdS .

Two body potential

- **The two-body potential** in this model takes a simple form

$$\mathcal{E}^{2\,\mathrm{body}}(m,n) =$$

$$\frac{2N_c}{5\lambda M} \times \frac{1}{|X_m - X_n|^2} \times \left[\frac{1}{2} + \mathrm{tr}^2\left(y_m^\dagger y_n\right) + \mathrm{tr}^2\left(y_m^\dagger y_n \left(-i\vec{N}_{mn} \cdot \vec{\tau}\right)\right) \right]$$

unit vector $\vec{N}_{mn} = \frac{\vec{X}_n - \vec{X}_m}{|X_n - X_m|}$

Two body forece between instantons

- The normalization is such that the average over the orientations of either of the instantons gives

$$\boxed{\langle \mathcal{E}^{2\,\mathrm{body}}(m,n)\rangle = \frac{N_c}{\lambda M}\frac{1}{|X_n - X_m|^2}}$$

- Note that the expression inside `[ ]' is always positive, so the two-body forces between the instantons are always **repulsive**, regardless of the instantons' SU(2) orientations.

Two body forece between instantons

- However, the **orientations** do affect the **strength of the repulsion**: two instantons with similar orientations repel each other 9 times stronger then the instantons at the same distance from each other but whose orientations differ by a 180 rotation (in SO(3) terms) around a suitable axis.

- The **total energy** of the system (including only the dominant two-body terms) is the sum over all pairs

$$\boxed{\mathcal{E}_{\text{tot}} = \sum_{n<m} \mathcal{E}^{2\,\text{body}}(m,n)\,.}$$

Generalizations of the dening instanton interactions

- It is natural to consider a **generalization** of the two-body potential which includes both the oriented interaction and the orientation independent potential.
- We therefore define

$$\mathcal{E}^{2\,\text{body}}(m,n;\alpha,\beta) = \frac{2N_c}{(1+2\alpha+2\beta)\lambda M}\frac{1}{|X_n-X_m|^2} \times \left[\frac{1}{2}+\alpha\,\mathrm{tr}^2\left(y_m^\dagger y_n\right)+\beta\,\mathrm{tr}^2\left(y_m^\dagger y_n(-i\vec{N}_{mn}\cdot\vec{\tau})\right)\right]$$

generalization parameters

- Notice that $\alpha = 0 = \beta$ gives the un-oriented potential and $\alpha = 1 = \beta$ gives back the ordinary two body potential

Generalizations of the defining instanton interactions

- α multiplies a term **independent** of the spatial interactions.
- For positive (negative) α perpendicular (parallel) spins of nearby neighbors are preferred, and the effect increases with increasing $|\alpha|$.
- The interaction β term involves a nontrivial coupling between the **orientations** and **directions** in coordinate space.
- Picking an instanton with unit orientation

(**y = 1**), positive (negative) β means that the orientation **y** of a neighboring instanton which is perpendicular (parallel) to the spatial link between the two instantons is preferred.

IR divergences

- In this work we determined the **crystal structure** and the **instanton orientation patterns** that minimize the total energy of the system.
- In order to understand our results, it is important to notice that the two-body interaction gives rise to a strong **long-distance (IR) divergence** in three dimensions.
- The potential due to a configuration of (large) size R behaves

$$\boxed{\int dr\, r^2\, \mathcal{E}^{2\,\mathrm{body}}(r) \sim \int dr\, r^0 \sim R}$$

- So it is linearly divergent.

IR divergences

- In several of these phases, **minimization of the energy** leads to nontrivial long distance correlations between the instanton orientations: for example, we obtain orientation structures which are **spherical** at long distances.
- Because of the divergence we need a **long-distance cutoff** in all our simulations and computations.
- Moreover, in the simulations, the long distance interactions lead to clustering of the instantons at the surface of the simulation volume if we only set a hard wall cutoff which forces the instantons to stay within the volume.
- The removal of this undesired effect necessitates the use of a **smooth external force** which pushes the instantons towards the center of the simulation.

Results

- Because of the long-distance divergence, however, there is no obvious “correct" choice for the external force for all configurations that we consider.
- A simple choice which is applicable to all configurations that we encounter is to take a force which sets the (locally averaged) **instanton density to be constant**.
- For most of the phase diagram this force matches with the (regularized) force due to a homogeneous density of instantons outside the simulation volume, i.e., the force due to the instantons left out of the simulation.
- In fact all our simulation results turn out to be insensitive to the precise choice of the force.

Methods of analyzing the lattices

- The results are obtained by using three different methods of analyzing the lattices of instantons:
- I. We perform **simulations** of ensembles of instantons of the order of O(10000) instantons subjected to the two body interactions between any two of them.
- II. We determine the **orientation patterns** based on the behavior of the two body potential for far apart instantons.
- In this range of distances between the instantons we take the **continuum limit** and ignore the lattice geometry. We compute the total energy of the system as a function of α and β, in particular we determine the associated lowest energy configuration.

Methods of analyzing the lattices

- III. We compute the energy difference between various pairs of geometrical and orientation structures by which we eventually determine the **phase diagram**.
- The computations of energy differences yield finite results since the divergences are cancelled out in the differences.

Resuts of the simulations of the basic setup

- **(1) In the non-orientation** case $\alpha = 0 = \beta$ the crystal structure is **face-centered-cubic (fcc).**

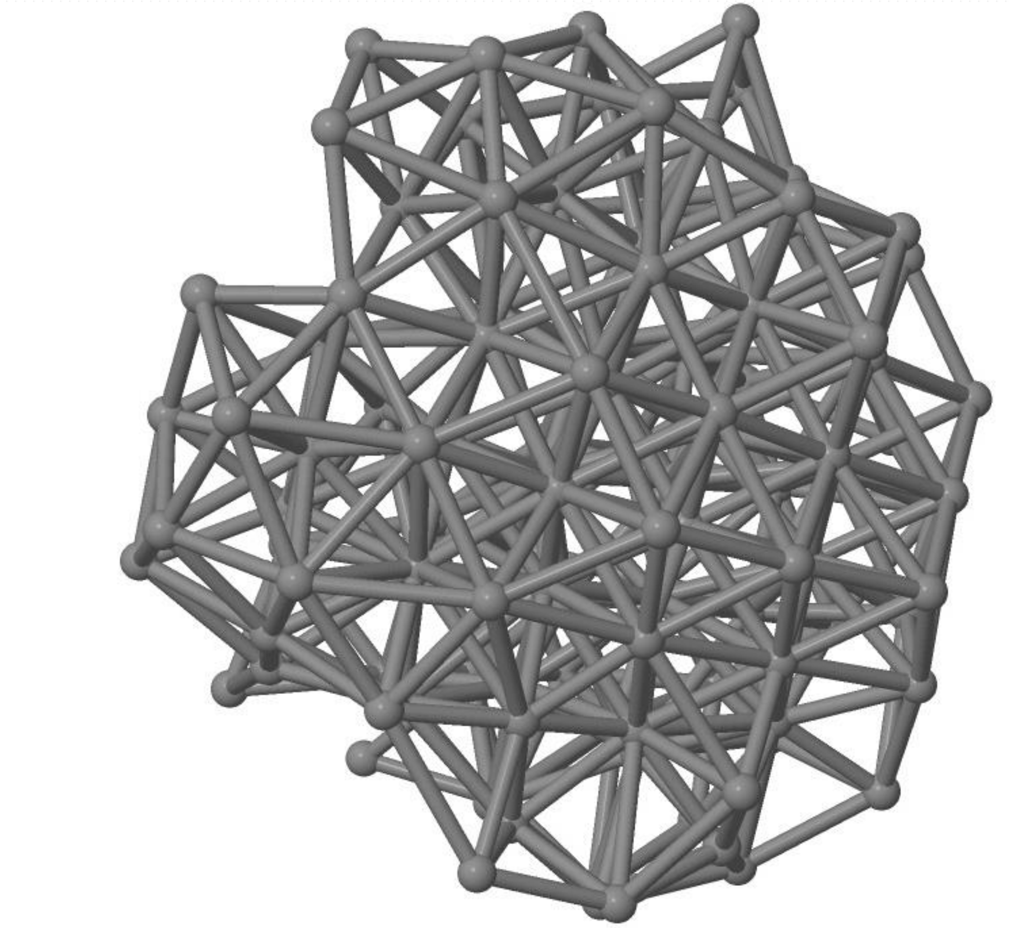

Resuts of the simulations of the basic setup

- **(2) The basic oriented** case $\alpha = 1 = \beta$ **is** face-centered tetragonal lattice with a large aspect ratio,1 i.e., fcc with one direction rescaled, breaking the cubic symmetry. The aspect ratio c is large: we find **c ~2.467**.
- That is, the instantons form clearly separated layers with two-dimensional square lattice structure.
- A sample of this structure is shown in the following fig.
- The two dimensional layers have **antiferromagnetic** structure. The orientations between the layers repeat in cycles of two.
- Overall, there are therefore four distinct and linearly independent orientations so that the set of orientations does not single out any direction. We call this class of orientation structures “**non-Abelian**".

The basic orientation setup α= 1 = β

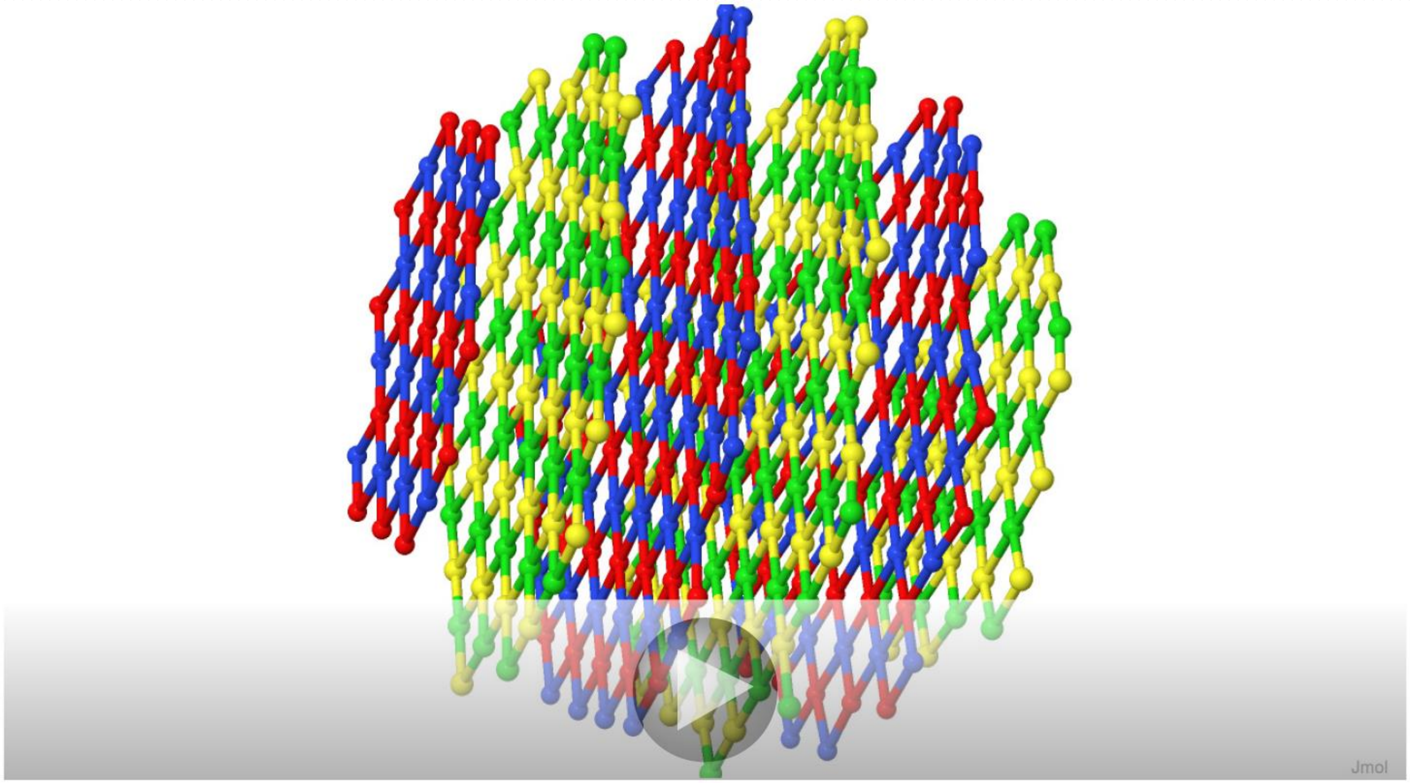

Figure 2: A sample of a simulation result for the oriented two-body interaction of 5d instanton dynamics (i.e. with $\alpha = \beta = 1$). The lattice is tetragonal with non-Abelian orientation structure. The colors show the four different orientations of the instantons. The figure was created by using the Jmol software [45]. An interactive 3D version of the figure can be viewed with Adobe Reader.

Oriented non-Abelian phase

- We have also revealed the **structure of the phase diagram** of the ensembles of instantons as a function of α and β .
- We identify the following phases:
- **(3) Oriented non-Abelian phase**. This phase contains crystals in the same class with the case $\alpha = \beta = 1$, i.e., the orientations span the whole four dimensional orientation space.
- We find this phase when

$\alpha > \beta$, $\beta > -1/8$, and $\alpha > \gamma_1 \beta$ with $\gamma_1 \sim 0.0575$.

Oriented non-Abelian phase

- The phase is further divided into **sub-phases** having different lattice and orientation structures, which can be classified into the following classes:

- (a) **Tetragonal/cubic** (fcc or fcc-related) lattices with “standard" orientation pattern
- (b) **Tetragonal/cubic** (fcc or fcc-related) lattices with “alternative" orientation pattern
- (c) **Hexagonal lattices**
- (d) **Simple cubic/tetragona**l lattices

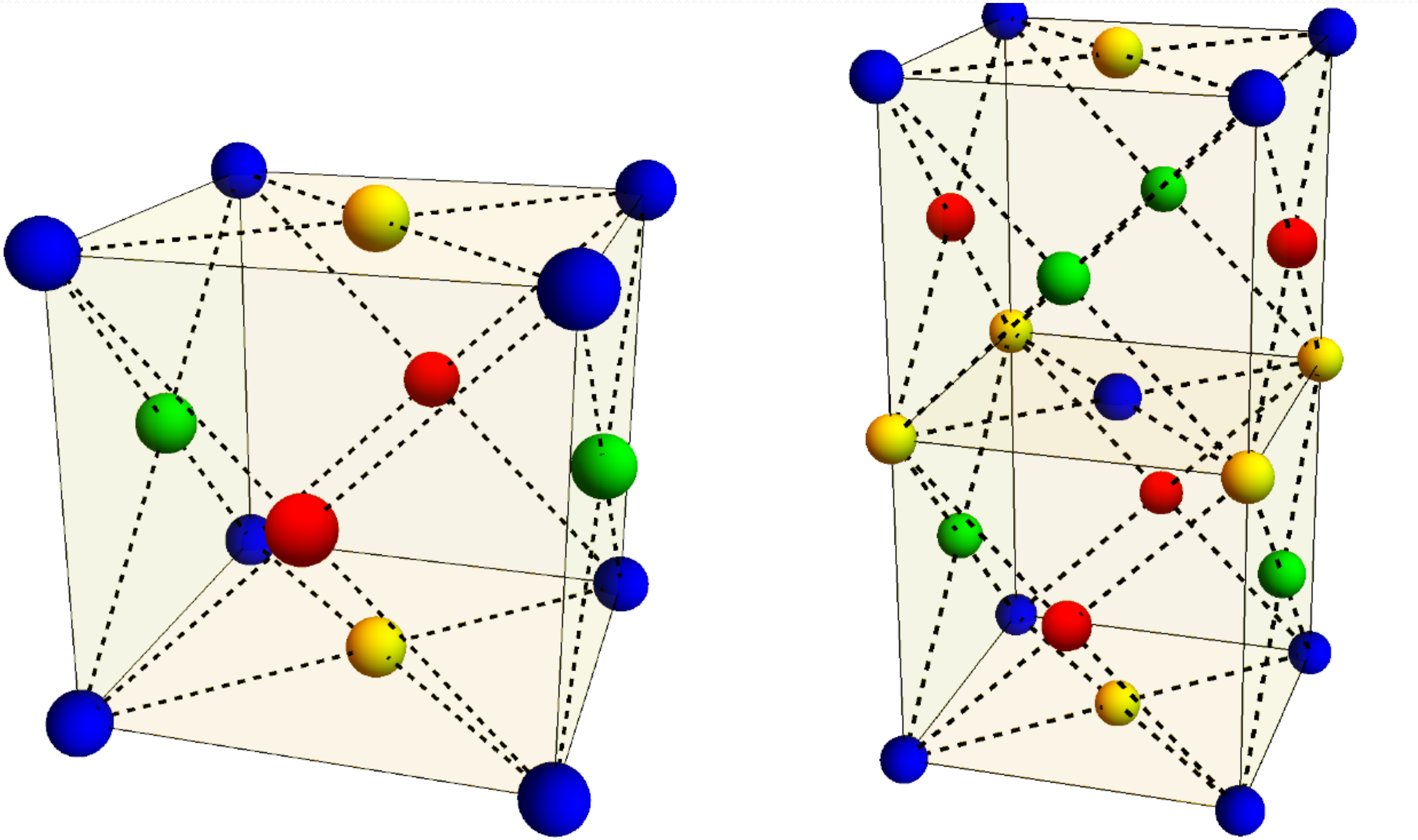

(a) fcc. (b) fcc with “alternative” orientations.

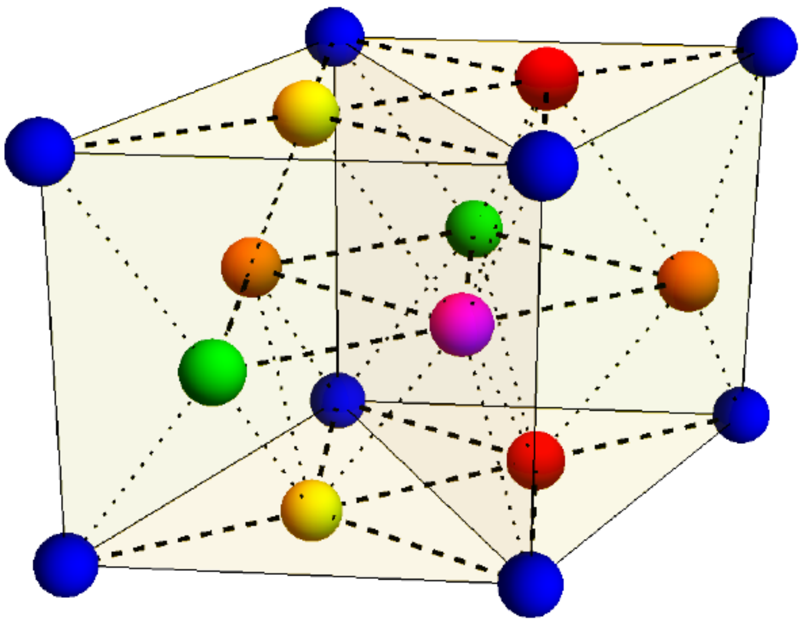

(c) Hexagonal.

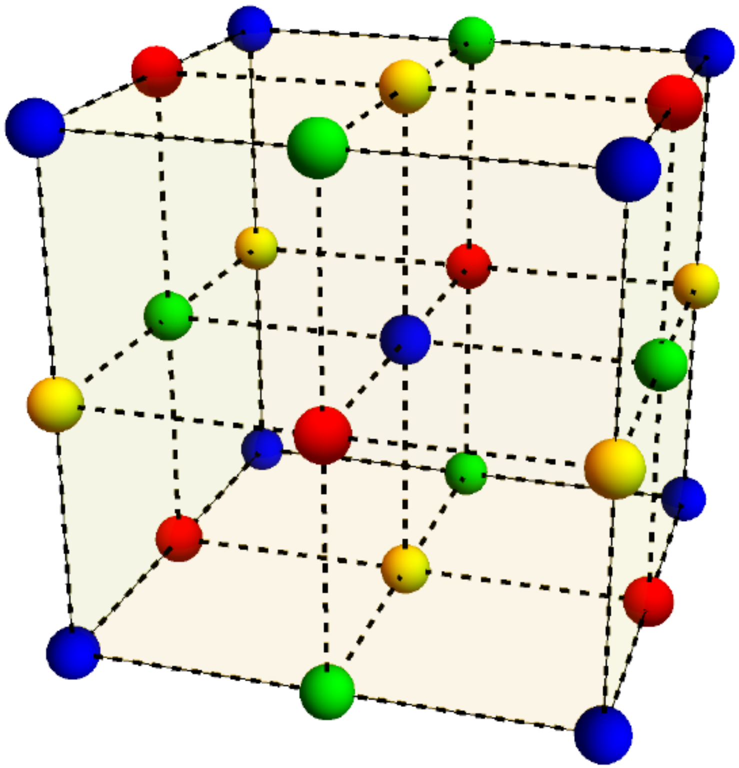

(d) Simple cubic.

Oriented non abelian phase

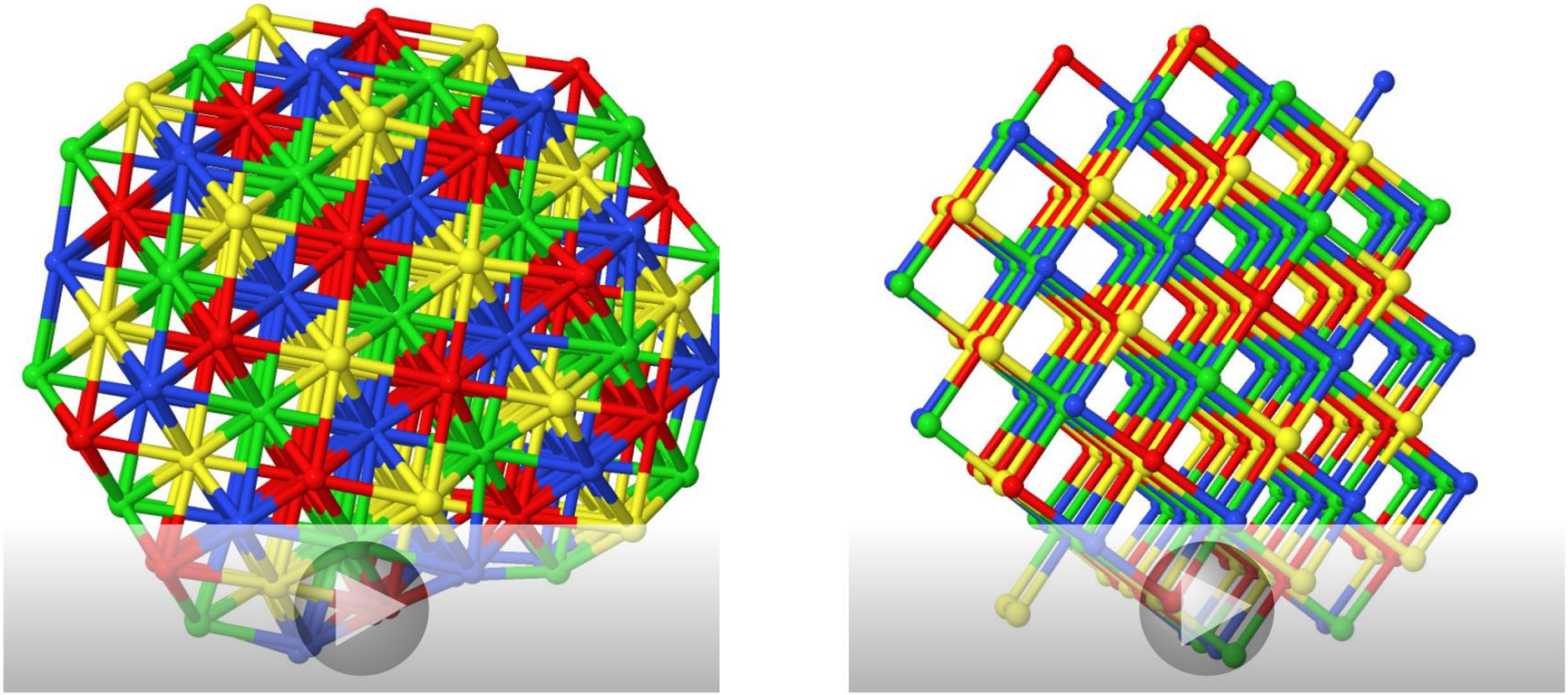

Figure 3: Generic lattice structures found in the non-Abelian phase. Left: A sample of fcc lattice from a simulation with 5000 instantons at $\alpha = 1$ and $\beta = 0.5$. Right: A sample of simple cubic lattice from a simulation with 6000 instantons at $\alpha = 0.5$ and $\beta = -0.03$.

Oriented non-Abelian phase

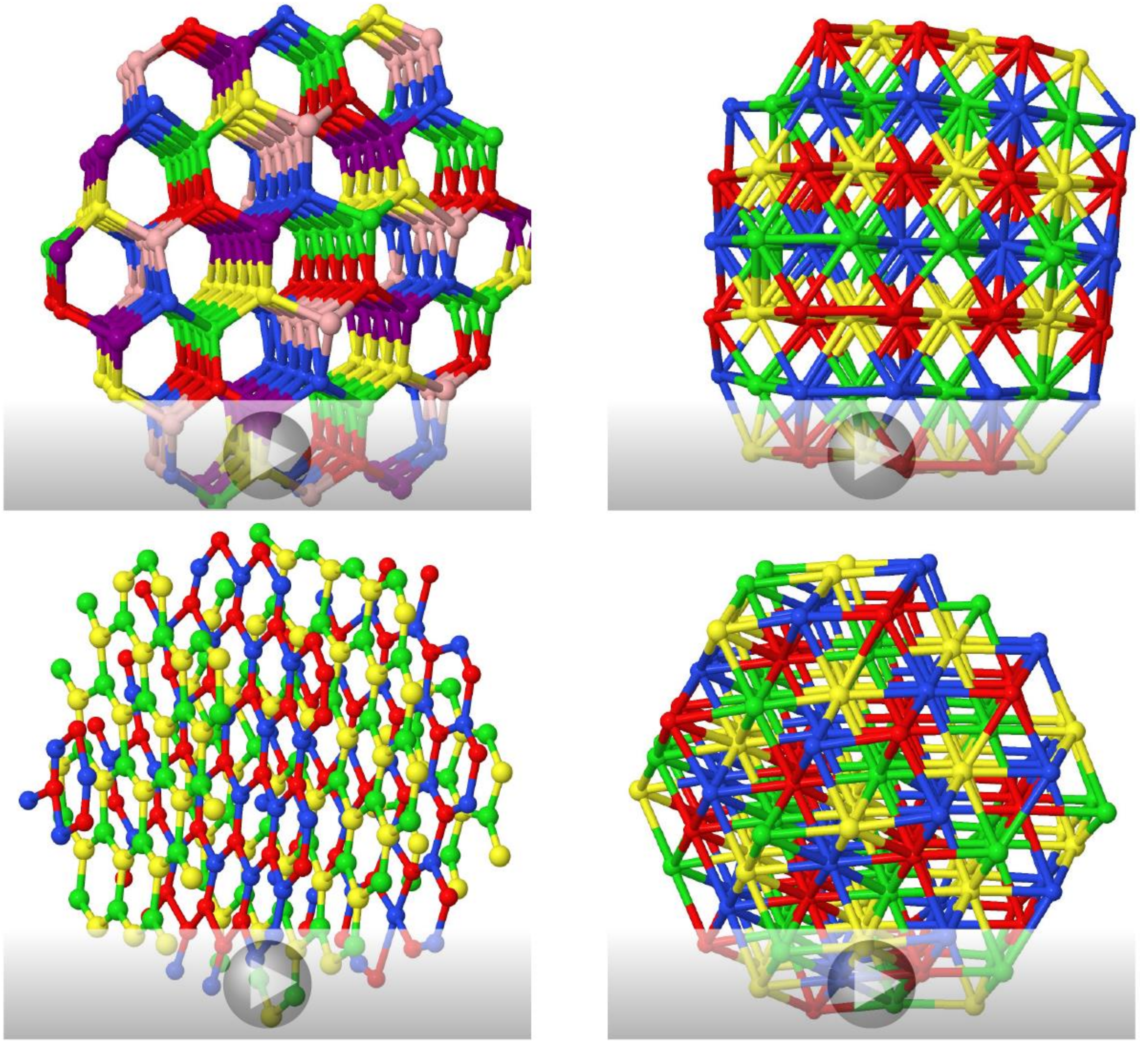

Figure 4: *Additional lattice structures found for* $0 < \alpha = \beta < 1$ *and for* $\beta = 0$. *Top left: A sample of hexagonal lattice from a simulation with 3000 instantons at* $\alpha = \beta = 0.4$. *Top right: A sample of a (nearly) bcc lattice from a simulation with 3000 instantons at* $\alpha = \beta = 0.07$. *Bottom left: A sample of a lattice with hexagonal antiferromagnetic layers from a simulation with 5000 instantons at* $\alpha = 10$ *and* $\beta = 10$. *Bottom right: A sample of a bcc lattice (with nonstandard orientation structure) from a simulation with 5000 instantons*

Anti-ferromagnetic phase

- **(4) Anti-ferromagnetic phase**. This phase is found when
  $\alpha < \beta < \Gamma\alpha$ with $\Gamma = 2{:}14$.

The orientation structure is locally antiferromagnetic: in domains of small size, only two different orientations appear.

- Globally the orientations are arranged spherically.
- The spatial lattice has a strong tendency of forming spherical shells.
- The two-dimensional lattice structure depends on α and β For $\alpha = O(1)$ and $\beta = O(1)$, the spherical shells have the structure of two-dimensional square lattice (with antiferromagnetic orientations).
- As and decrease, the lattice changes to **rhombic**. For small values, $\alpha = O(0.1)$ and $\beta = O(0.1)$, the layers are closer to **triangular** and the spatial structure is locally close to **bcc**.

Spherical and global ferromagnetic phase

- **(5) Spherical ferromagnetic phase**. In the sector $\beta > \Gamma\alpha > 0$,
- we find a pattern which is **locally fcc and ferromagnetic**, all nearby orientations are (almost) the same.
- However **globally** the orientations form a **spherical structure**. The simulations indicate that the lattice structure is independent of α and β within the phase.
- **(6) Global ferromagnetic phase**. In the area of negative , precisely limited by the conditions

$$\boxed{-1/8 < \alpha < 0, \quad \beta > -1/8, \quad \alpha < \gamma 2\, \beta \quad \gamma 2 \sim 0.543}$$

we find a global **ferromagnetic** pattern.

That is, the lattice is (locally and globally) fcc and all orientations are aligned.

Spherical and global ferromagnetic phase

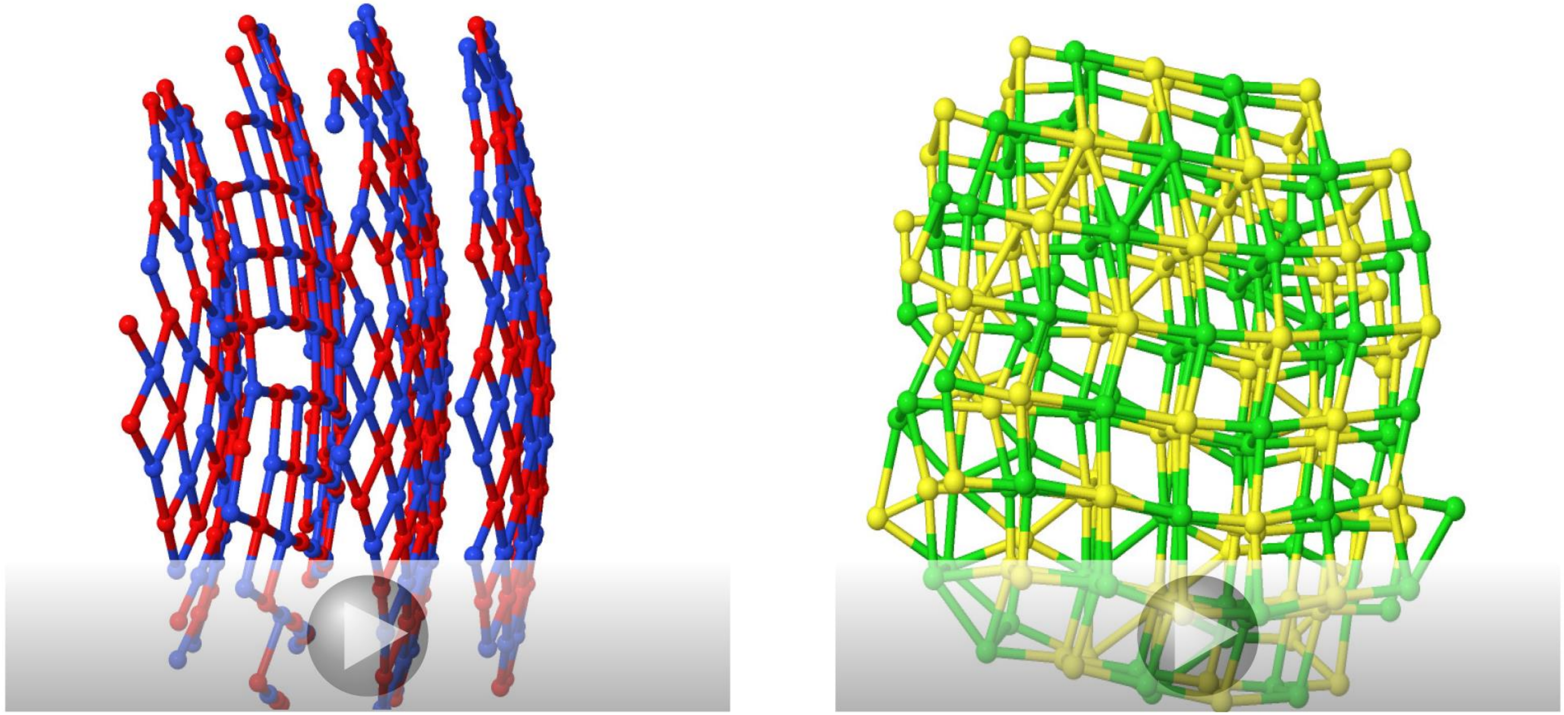

Figure 5: *anti-ferromagnetic spherical lattices found for* $0 < \alpha < \beta$. *Left: A sample with two-dimensional square lattice layers from a simulation with 15000 instantons at* $\alpha = 2/3$ *and* $\beta = 1$. *Right: A sample with two-dimensional rhombic layers from a simulation with 15000 instantons at* $\alpha = 0.1$ *and* $\beta = 0.15$.

Ferromagnetic egg phase

- (7)Ferromagnetic egg phase. In the remaining corner of the phase diagram, i.e., whe

$$\boxed{\gamma_2 \beta < \alpha < \gamma_1 \beta \quad \text{and } \beta > -1/8,}$$

- we find a special ferromagnetic crystal. It is again **locally fcc**, and the interior of the sample orients as a global **ferromagnet**, but there is crust of finite width where the orientations obey a **global spherical alignment.**

Phase diagram

- We draw the **phase diagram** of the **non-Abelian lattices** on the α and β -plane.
- The result for the phase diagram is shown in fig.
- In the figure the blue, red, green, and yellow colors indicate crystals (a), (b), (c), and (d) , respectively.
- The brightness of the color is given by the aspect ratio, with brighter (darker) shades corresponding to lower (higher) values.
- The largest solid blue domain is fcc, i.e., aspect ratio is $c = 1$, and the large yellow domain is simple cubic. In all the other domains, the aspect ratio varies with α and β.

Phase diagram

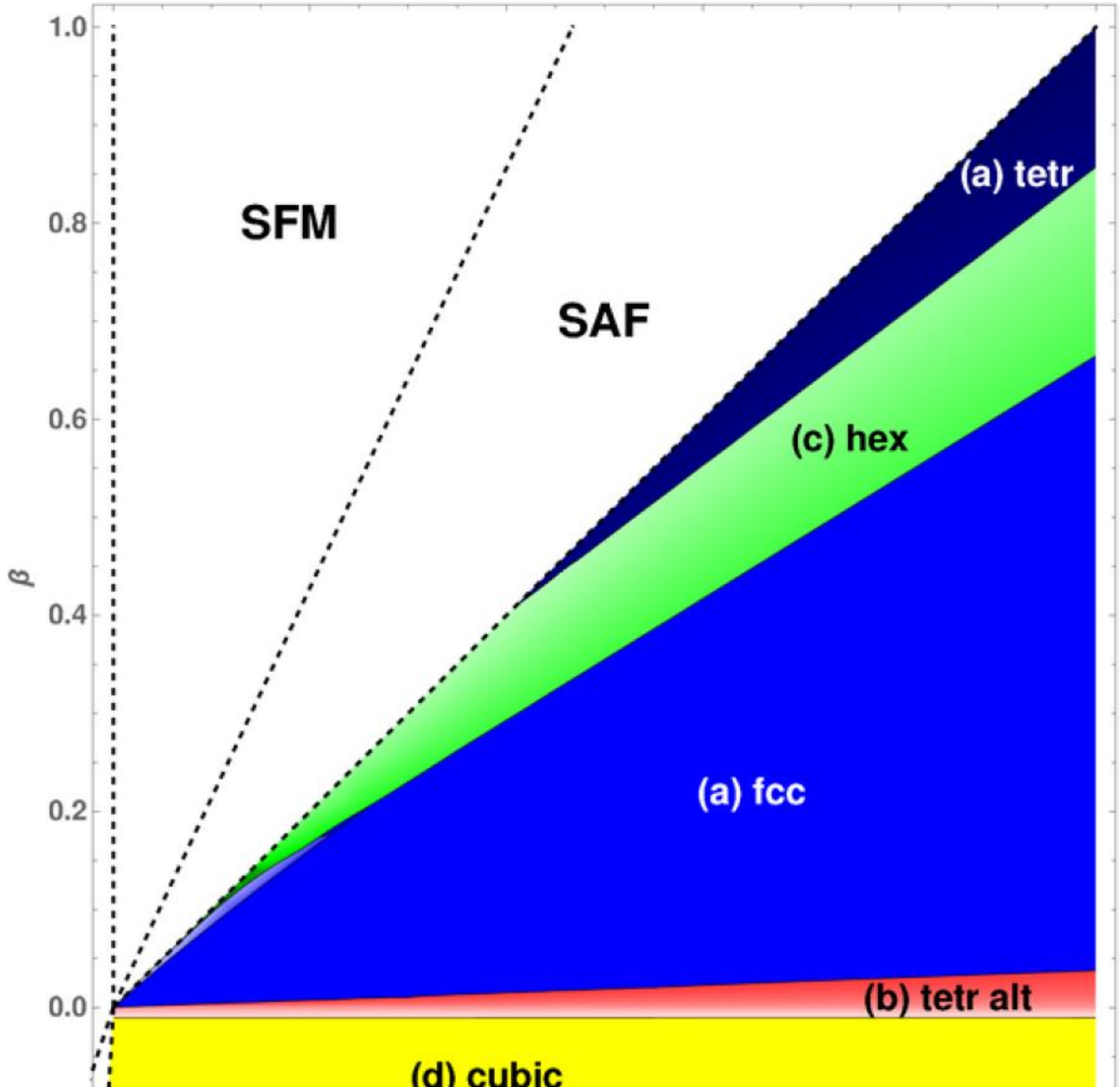

Phase diagram

- We continue by analyzing the phase diagram close to the critical lines in the simulations in Sec. 3, starting from the results near the diagonal,

$$0 < \alpha = \beta < 1.$$

- We show the phase structure in this region in the following fig. where we switched to angular coordinates and show the \radial" coordinate in log scale

Phase diagram

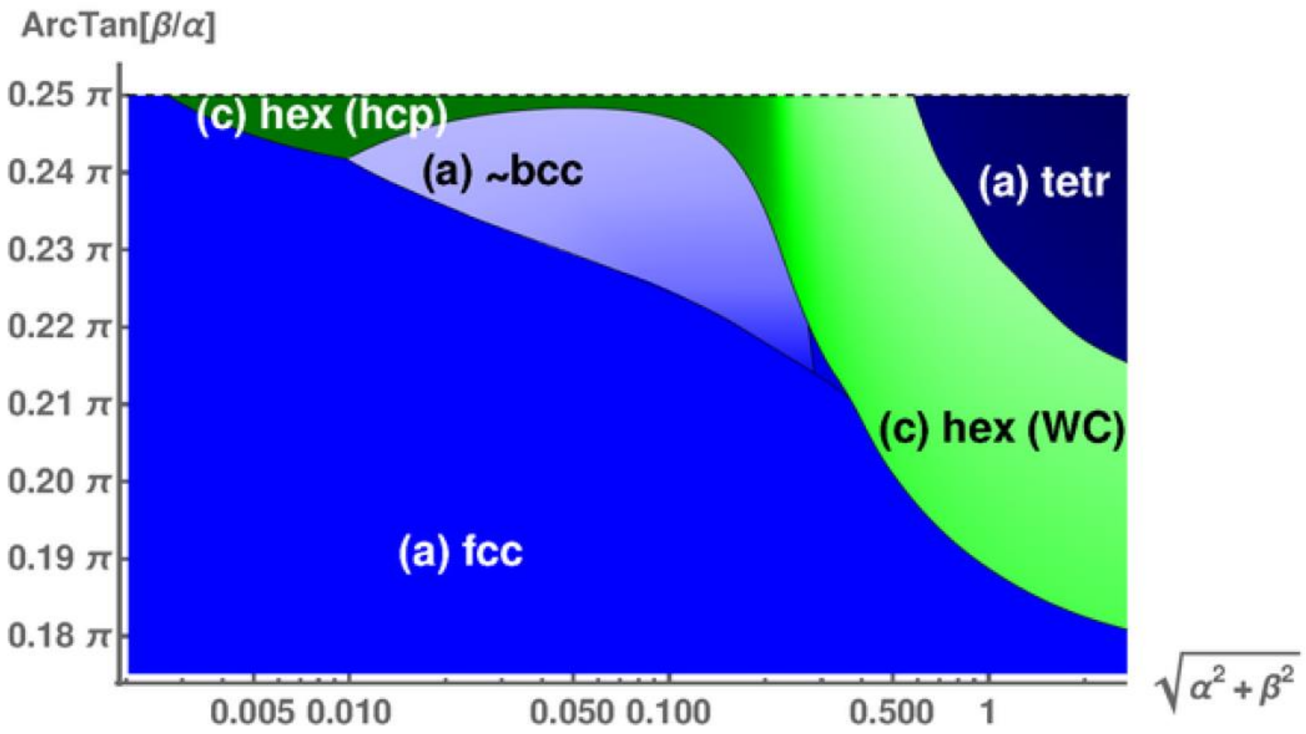

Figure 11: *The details of the phase diagram near* $\alpha = \beta$. *We use angular coordinates and*

Phase diagram

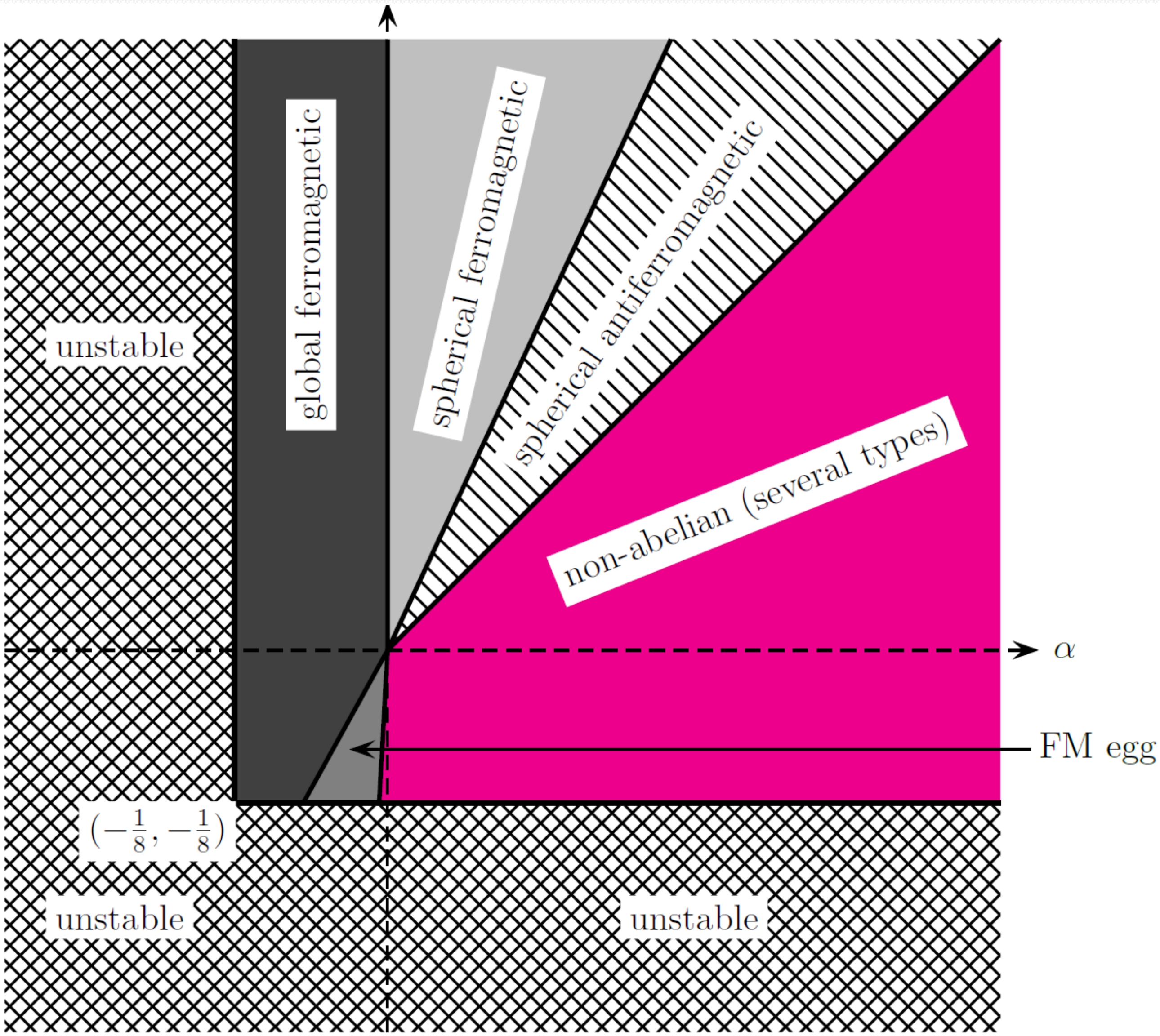

Figure 8: Orientation phase diagram of 3D quasi-instanton matter, regardless of lattice structure.

Open questions

- The systems discussed in this paper are at zero temperature. It will be interesting to consider instead lattices of instantons (Torons) at **finite temperature**.
- Another obvious generalization is transforming the avor symmetry U(2) ! **U(Nf)** and in particular the eight-fold symmetry Nf = 3. In the opposite direction one would like to explore also the breaking of the isospin symmetry
- In recent years there has been an effort to apply holography to the study of **neutron starts and their mergers.** It will be interesting to understand if and how taking crystal structures rather than the liquids changes the picture of neutron stars. Moreover, our analysis included the spherical fermionic and anti-fermionic structure. These phases may be relevant to the nuclear structure of neutron stars that obviously are **spherically symmetric.**